Published in final edited form as:
Alcohol Clin Exp Res. 2011 November ; 35(11): 2063–2074. doi:10.1111/j.1530-0277.2011.01557.x.

Effects of early postnatal exposure to ethanol on retinal ganglion cell morphology and numbers of neurons in the dorsolateral geniculate in mice

Ilknur Dursun[1], **Ewa Jakubowska-Doğru**[1], **Deborah van der List**[2], **Lauren C. Liets**[2], **Julie L. Coombs**[2], and **Robert F. Berman**[3]

[1]Department of Biological Sciences, Middle East Technical University, 06531 Ankara, Turkey

[2]Department of Neurobiology, Physiology, and Behavior, UC Davis, Davis, CA 95616

[3]Center for Neuroscience & Department of Neurological Surgery, UC Davis, Davis, CA 95616

Abstract

Background—The adverse effects of fetal and early postnatal ethanol intoxication on peripheral organs and the central nervous system are well documented. Ocular defects have also been reported in about 90% of children with Fetal Alcohol Syndrome (FAS), including microphthalmia, loss of neurons in the retinal ganglion cell layer (GCL), optic nerve hypoplasia and dysmyelination. However, little is known about perinatal ethanol effects on retinal cell morphology. Examination of the potential toxic effects of alcohol on the neuron architecture is important since the changes in dendritic geometry and synapse distribution directly affect the organization and functions of neural circuits. Thus, in the present study estimations of the numbers of neurons in the GCL and dorsolateral geniculate nucleus (dLGN), and a detailed analysis of RGC morphology were carried out in transgenic mice exposed to ethanol during the early postnatal period.

Methods—The study was carried out in male and female transgenic mice expressing Yellow Fluorescent Protein (YFP) controlled by a Thy-1 (thymus cell antigen 1) regulator on a C57 background. Ethanol (3 g/kg/day) was administered to mouse pups by intragastric intubation throughout postnatal days (PD) 3–20. Intubation control (IC) and untreated control (C) groups were included. Blood alcohol concentration (BAC) was measured in separate groups of pups on PD3, PD10, and PD20 at 4 different time points, 1, 1.5, 2 and 3 h after the second intubation. Numbers of neurons in the GCL and in the dLGN were quantified on PD20 using unbiased stereological procedures. Retinal ganglion cell morphology was imaged by confocal microscopy and analyzed using Neurolucida software.

Results—Binge-like ethanol exposure in mice during the early postnatal period from PD3 through PD20 altered RGC morphology and resulted in a significant decrease in the numbers of neurons in the GCL and in the dLGN. In the alcohol exposure group, out of 13 morphological parameters examined in RGCs, soma area was significantly reduced and dendritic tortuosity significantly increased. After neonatal exposure to ethanol a decrease in total dendritic field area and an increase in the mean branch angle were also observed. Interestingly, RGC dendrite elongation and a decrease in the spine density were observed in the IC group, as compared to both ethanol-exposed and pure control subjects. There were no significant effects of alcohol exposure on total retinal area.

Corresponding Author: Robert F. Berman, Ph.D., Center for Neuroscience & Department of Neurological Surgery, University of California Davis, Davis, CA 95616, Fax: 530-754-5102, Voice: 530-754-5102, rfberman@ucdavis.edu.

Conclusion—Early postnatal ethanol exposure affects development of the visual system, reducing the numbers of neurons in the GCL and in the dLGN, and altering RGCs' morphology.

Keywords

postnatal ethanol; yellow fluorescent protein (YFP) mice; Retinal ganglion cell (RGC) morphology; stereological cell counts

Introduction

Perinatal (pre- and early postnatal) alcohol exposure affects a variety of organ systems in both humans and laboratory animals. Fetal Alcohol Syndrome (FAS) and the less severe Fetal Alcohol Spectrum Disorders (FASD) are described as a set of specific human birth defects related to maternal alcohol consumption during pregnancy characterized by pre- and postnatal growth retardation, craniofacial defects and central nervous system (CNS) dysfunctions (Bruce et al., 2009; Jones and Smith, 1973; Lemoine et al.,1968).

Both human and animal research has shown reductions in brain weight and microencephaly resulting from prenatal exposure to alcohol (Jones et al., 1973; Clarren et al., 1978; Streissguth et al., 1980; Pierce and West, 1986; Bonthius and West, 1990; Tran et al., 2000). Neuronal loss is one of the most common deleterious effects of fetal and early postnatal exposure to alcohol on the CNS, and several studies have reported reduced numbers of neurons and fibers within different brain regions including the hippocampus (Barnes and Walker, 1981; Gonzalez-Burgos et al., 2006; Livy et al., 2003; Miki et al., 2003; Moulder et al., 2002) cerebellum (Goodlett et al.,1998; Goodlett and Eilers, 1997; Miki et al.,1999; Thomas et al., 1998), and corpus callosum (Qiang et al., 2002; Riley et al., 1995). Perinatal alcohol exposure also produces a variety of types of damage to the visual system. Ocular defects have been reported in about 90% of children with FAS suggesting that ocular structures are sensitive to alcohol exposure during their development (Strömland, 1987). Because of the marked similarity among the eyes of all vertebrates, it is not surprising that microphthalmia, retinal ganglion cell loss, optic nerve hypoplasia, delayed myelination and/or reduced myelin thickness in the optic nerve fibers have all been observed after ethanol exposure during the embryonic development in fish (Dlugos and Rabin, 2007; Kashyap et al.,2007; Matsui et al., 2006), chick (Chmielewski et al. 1997; Tufan et al., 2007), mouse (Ashwell and Zhang, 1994; Cook et al., 1987; Kennedy and Elliott, 1986; Parson et al., 1995; Parson and Sojitra, 1995), rat (Harris et al., 2000; Pinazo-Duran et al., 1993, 1997; Philips et al., 1991; Pons et al., 2007; Strömland and Pinazo-Duran, 1994) and monkey (Clarren et al., 1990).

The adverse effects of fetal alcohol exposure are mediated by multiple mechanisms and depend on dose, pattern, and timing of exposure with different tissues and organs showing different vulnerability to ethanol effects (Berman and Hannigan, 2000; Guerri, 2002; Mooney and Miller, 2007). In mice, even a single exposure to ethanol, mimicking a 'binge' abuse of alcohol, during critical period of ocular ontogeny (E13) was reported to cause adverse ocular changes (Ashwell and Zhang, 1994; Kennedy and Elliott, 1986). Also during the early postnatal period, a single ethanol intoxication episode was shown to trigger apoptosis of retinal ganglion cells as well as of neurons at higher levels of the visual system. Tenkova et al., (2003) observed significant retinal ganglion cell (RGC) degeneration in rat pups after a single exposure to ethanol applied at various postnatal ages within the first postnatal weeks of life. The loss of RGCs was especially pronounced during a relatively narrow developmental time window from PD 1 to PD 4. The period of peak sensitivity for the higher order visual neurons was defined as postnatal days 4–7. These results suggest that in rodents the visual system shows increased vulnerability to the adverse effects of ethanol

during the first 10 postnatal days, the time corresponding to the third trimester in human and known as the brain growth-spurt period (Dobbing and Sands, 1979; Rice and Barone, 2000). However, RGCs development is not completed until PD20 when the dendritic arbor is finally shaped (Chalupa and Williams, 2008 pp194). Therefore, it is also important to examine the potential adverse ethanol effects on developing retina over the extended postnatal period covering the whole process of RGCs maturation.

Most recent studies have examined ethanol effects on the developing visual system and focused on alcohol-induced changes in cell numbers and optic nerve myelination. Therefore, little is known about the potential effects of fetal and early postnatal ethanol exposure on the morphology of retinal neurons. Morphological effects have been reported in other brain areas. For instance, Qiang et al., (2002) reported abnormal dendritic arborization of corpus callosum projection neurons after ethanol treatment administered during the second trimester in rats. Examination of the potential toxic effects of drugs including alcohol on the neuron architecture is important as it is well known that the neurons' dendritic arborization and the synapse distribution along the neurites have profound effects on the organization and functions of local neural circuits.

Previous studies have provided detailed descriptions of the morphological features of RGCs in adult mice (Badea and Nathans, 2004; Coombs et al., 2006; Jeon et al., 1998; Kong et al., 2005; Sun et al., 2002). Additional studies have also traced the development of RGCs during the early postnatal period in mice (Coombs et al., 2007; Diao et al., 2004). These data constitute a frame of reference for the current studies on the effects of ethanol intoxication on retina development.

The present study was designed to investigate the effects of the early postnatal exposure to ethanol on the morphology of RGCs and on the numbers of neurons within the retinal ganglion cell layer and dorsolateral geniculate nucleus of the thalamus (dLGN) in transgenic mice expressing yellow fluorescent protein (YFP).

MATERIALS AND METHODS

Subjects

Both male and female transgenic mice expressing Yellow Fluorescent Protein (YFP) controlled by a Thy-1 (thymus cell antigen 1) regulator on a C57 background (YFP-H line, Jackson Laboratory, Bar Harbor, ME, USA; Feng et al., 2000) were used in this study. The YFP-H line expresses YFP in most types of RGC's identified and are visible by postnatal day 8 (Coombs et al., 2006, 2007). Pups used in these experiments were randomly selected from different litters. All procedures were approved by the Institutional Animal Care and Use Committee of the University of California, Davis (IACUC). Animals were housed in IACUC approved animal facilities under controlled environmental conditions.

Neonatal Treatment

The newborn YFP pups were divided into 3 groups; alcohol treated (A), intubation controls (IC), and non-intubated controls (C). The day of birth was designated as Postnatal Day (PD) 0. Pups in group A were intubated each day from PD 3 to PD 20 with 3 g/kg body weight ethanol delivered in a 0.02 ml/g volume of artificial enriched milk. The milk formula was prepared after Kelly and Lawrence (2008) and contained evaporated milk, a custom mix of minerals (ZnSO4, CuSO4, FeSO4, MgCl, KCl) and vitamins (BioServ, Beltsville, MD), Supro 710 protein power (Ralston Purina Co., St. Louis, NJ), corn oil, methionine, tryptophan, calcium phosphate dibasic, and deoxycholic acid. The alcohol dose of 3 g/kg body weight has been used in previous rodent studies and shown to result in adverse effects on brain morphology and behavior (Tran et al., 2000; Green et al., 2006).

The alcohol solution was divided into two equal doses given to pups two hours apart. Two hours after the second intubation, pups were reintubated with 0.02 ml/g of the milk solution alone. The pups were intubated at the same time each morning. Each day one hour before intubation the litter was taken from the dam and placed on a heating pad maintained at 37 °C. Between intubations, the pups were returned to the dam. Intubations were carried out using PE-10 tubing (Clay Adams Brand, Becton Dickinson) lubricated with corn oil and attached to a 1cc insulin syringe filled with milk with or without alcohol. The length of the tube was measured from the mouth to the stomach and marked. The PE-10 tube was carefully inserted down the esophagus into the stomach and a measured amount of solution was given immediately. Pups from the IC group, a control for possible intubation-induced stress effects, were intragastrically intubated in the same manner as those from the A group, but received neither ethanol nor milk. The non-intubated control group (C) was weighed daily with no additional treatment.

Blood Alcohol Concentration

Blood alcohol concentration (BAC) was measured in a separate group of pups on PD3, PD10, and PD20 at 4 different time points, 1, 1.5, 2 and 3 h after the second intubation. On PD 3 and PD 10, pups were anesthetized in an ice bath until movement stopped then decapitated and blood collected. On PD20, 10μl of tail blood was collected into heparinized capillary tubes. BAC was determined using an oximetric procedure (Helfer et al., 2009) with an Analox GL5 Alcohol Analyzer (Analox Instruments, Lunenburg, MA). Between 2 and 4 different pups were sampled for each PD and each time point.

Retina collection

On PD20, after the last intubation, the pups from A, IC, and C groups were euthanized with a lethal i.p. dose (0.1 ml) of Fatal Plus (Vortech Pharmaceuticals). After enucleation, the cornea and lens were removed. The eyecup was fixed for 2 h in 4% paraformaldehyde (PFA) in phosphate buffered saline (PBS) and then washed and stored in PBS until processed for immunohistochemistry. Before removing the retina from the sclera, a notch was made to identify the nasal retina.

Immunohistochemistry

Fixed retinas were blocked for 2 h in a blocking solution containing 10% normal donkey serum (Jackson Immuno Research), 2% bovine serum albumen (Jackson Immuno Research, West Grove, PA), 0.3% Triton X-100 in PBS (Fisher Scientific, Atlanta, GA). The following primary antibodies were diluted in fresh blocking solution: rabbit anti-green fluorescent protein (GFP) (1:500; Invitrogen, Carlsbad, CA) and a goat anti-choline acetyltransferase (1:50; Chemicon International, Temecula, CA). The retinas were incubated in the primary antibody for 3–4 days at 4 °C. After washing three times in PBS, the retinas were incubated for 2 h at room temperature in secondary antibodies Alexa-488 and Alexa 568 (1:500; Invitrogen, Carlsbad, CA) diluted in PBS. Finally, retinas were rinsed three times in PBS and incubated overnight in DAPI (1:500; KPL, Gaithersburg, MD). Radial cuts were made to flatten the retina, with careful note taken to the nasal identifying notch. Flattened retinas were then mounted on a glass slide, coverslipped with PBS as the mounting media and sealed with Depex (Electron Microscopy Sciences, Hatfield, PA).

Imaging and morphometric measures

The retinal ganglion cells that had obvious axons were chosen for imaging. High-resolution three-dimensional images were taken using an Olympus Fluoview 500 confocal microscope with the following parameters; x and y =1024 × 1024 pixels, and two images averaged at each focal plane. Each confocal image stack of individual retinal ganglion cells was traced

using Neurolucida software (Microbrightfield, Williston, VT). Fourteen parameters were measured and analyzed as described in Coombs et al., 2006, including soma size, dendritic field size, total dendritic length, number of dendrites, number of dendritic branches, branch order, mean internal branch length, mean terminal branch length, branch angle, number of dendrites, spine density, tortuosity, dendrite diameter and symmetry. A photomicrograph of a (A) representative yellow fluorescent (YFP) retinal ganglion cell and (B) the morphological features measured are shown diagrammatically in Figure 1.

Cell Counting Procedures

Cell counting was done on retinas obtained from different animals as follows: A (n=7), IC (n=7), C (n=6). Free-floating whole retinas were stained with 0.1% cresyl violet for 6 minutes then twice rinsed with PBS for 20 seconds each time. Stained whole-mount retinas were mounted on a glass slide in PBS, coverslipped and sealed with Depex (Electron Microscopy Sciences, Hatfield, PA). Using a 20X objective on a Nikon E600 microscope (Nikon Instruments Inc., Melville, NY), a contour line was drawn around each retina to define the region of interest (ROI) and a 100X oil-immersion lens was then used for individual cell counting (i.e., 1000 magnification). The counting frame was set at 25μm with a grid size of 500μm. Unbiased stereological analysis of the number of retinal ganglion and amacrine neurons in the retinal ganglion cell layer was then carried out using StereoInvestigator software (Microbrightfield, Williston, VT).

Stereological procedures were also used to estimate the number of dLGN neurons. Brains were removed immediately after the eye dissection on PD20, post-fixed for 3 days in 4% paraformaldehyde, cryoprotected in 10% sucrose solution for 1h, in 30% sucrose solution for another 24h, and then frozen in 30% sucrose. Brains were serially sectioned in the coronal plane at 50μm on a sliding microtome (American Optical model 860, Buffalo, NY). Sections were mounted on slides, air dried and stained with Cresyl violet. On each section, the dLGN was outlined using a 10X objective, and neurons were counted under oil immersion using a 100X objective (i.e., 1000 magnification). The counting frame was set at 20μm with a grid size of 100μm. Every 2nd tissue section was counted through the entire dLGN. Tissue section thickness was measured for each counting frame and the number-weighted section thickness was used when calculating numbers of neurons. A fixed dissector height of 10 μm was used in each counting step, and a guard height of 2 μm was used to avoid artifacts at the sectioning surface. The numbers of neurons within the dLGN were counted by unbiased stereological methods, using the optical fractionator probe in the StereoInvestigator software (Microbrightfield, Williston, VT). The optical fractionator is unaffected by tissue shrinkage that takes place during tissue preparation (West, 1993).

Statistical Analyses

From all measures group means ± SEM were calculated. The data were analyzed with treatment (i.e., A, IC, and C) as the independent factor. A one way ANOVA for the number of neurons in the retina and dLGN, and a repeated measure ANOVA for body weight were carried out. A conditional hierarchical linear model was employed for analysis of morphometric parameters of RGCs. The three-level hierarchical linear model consisted of three variance components parameters: the treatment-to-treatment variability (fixed effects part), retina-to-retina variability (random effects part), and cell-to-cell variability (random effects part). The Tukey HSD and the Differences of Least Squares Means tests were used for *post hoc* analysis of the data. The statistical packages SAS and SPSS 16 (Chicago, IL) were used.

RESULTS

Body weight

The pups' mean body weight (± SEM) was analyzed throughout PD3-PD20 for A (n=10), IC (n=7), and C (n=8) groups. A two-way repeated measures ANOVA (treatment × days) yielded significant day effect ($F_{(17,374)}$ = 374.68, p<0.00) confirming a steady increase in the pups' body weight throughout the first 10 postnatal days. There was no statistically significant effect of alcohol treatment on body weight (Figure 2).

Blood Alcohol Concentration

Figure 3 shows BAC concentrations measured at 4 time points after the second intubation on PDs 3, 10 & 20. The peak BAC was observed 1–1.5 h after the second intubation, at 298 ± 5.9, 256 ± 22.7, and 156 ± 4.1 mg/dl for PD3, PD10, and PD20, respectively. The mean BAC was inversely proportional to the pups' age.

Retina Area and Number of Neurons in the Retinal Ganglion Cell Layer and in the Dorsolateral Geniculate Nucleus (dLGN)

At PD20, in the ethanol-treated group, there was no change in the total retinal area compared to controls (Fig. 4A). However, the number of neurons in the retinal ganglion cell layer (Fig. 4B) was significantly affected by alcohol exposure ($F_{(2,18)}$= 5.86, p=0.012), and individual group comparisons confirmed that there were significantly fewer neurons in group A compared to the IC and C groups (p=0.02 and p=0.03, respectively). The two control groups did not differ significantly (Fig.4B). For the dLGN cell count (Fig. 4C) there was a significant main group effect ($F_{(2,19)}$= 3.76, p=0.044). However, post hoc comparisons revealed that only the difference between A and IC groups was statistically significant (p=0.035).

Morphometric analyses of Retinal Ganglion Cells (RGC)

The numbers of traced ganglion cells were as follows: Alcohol (n=104), Intubation Control (n=81), Control (n=108). The number of animals used in each treatment group and mean number of RGC's per animal used for counting were as follows: Group A (n=4), mean = 26; Group IC (n=5), mean = 16.2; and C group (n=5), mean = 21.6.

Somal area—As seen from Fig. 5A, alcohol treatment significantly reduced the mean soma area of retinal ganglion neurons ($F_{(2,16)}$= 4.25, p=0.033). Individual group comparisons showed that mean soma area for Group A was significantly smaller compared to both control groups (p=0.017 and p=0.031, for IC and C group, respectively). The two control groups did not differ significantly. In all three groups, ganglion cell soma area showed a normal frequency distribution with a peak at 250 μm^2 for alcohol-treated pups and 350 μm^2 for control subjects (Fig. 5B).

Dendritic field area—The mean dendritic field area was also smaller in the alcohol group as compared to Groups C and IC (Fig. 6A). Statistical analysis showed that the treatment effect just failed to reach statistical significance ($F_{(2,16)}$=3.30, p=0.06). Nevertheless, in view of the significant decrease in soma area for Group A (see Fig. 5A), individual group comparisons were carried out on dendritic field area. This analysis showed that the dendritic field area was significantly smaller for Group A compared to Group IC (p=0.02). The difference between Groups A and C was not significant (p=0.09), and the two control groups did not differ significantly (p=0.4). As seen from Fig. 6B, in the ethanol-exposed pups, neurons with dendritic fields within the range between 20000 – 30000 μm^2 constituted the

largest group of ganglion cells. In contrast, in the control groups, the largest group of ganglion cells had dendritic fields within the range between 30000 – 40000 μm^2.

Total Dendritic length—Analysis of dendritic length (Fig. 7A) showed a significant main effect of treatment ($F_{(2,16)}$=3.64, p<0.05). Post hoc analysis showed that the mean dendrite length in the IC group was significantly greater than that in either the A or C groups (p=0.034 and p=0.026, respectively) with no significant difference between Groups C and A. Differences were also observed between treatment groups for the dendrite length frequency distribution (Fig. 7B). In control pups, the predominant dendrite length was between 35000 and 40000 μm. In alcohol group, the typical dendritic length fell within a broader range of values, between 35000 and 45000 μm. In contrast, in the IC group of pups the distribution of dendritic length showed two peaks, one at 40000–45000 and the second at 55000–60000 μm (see Fig. 7B).

Dendritic tortuosity—Dendrite tortuosity was estimated as the ratio of the length along each dendritic branch and the length of the straight line drawn between the two nodes that define the branch. As shown in Figure 8A, the overall group effect was highly significant ($F_{(2,16)}$=16.76, p=0.0001). Individual group comparisons showed that dendritic tortuosity was significantly higher in Group A compared to groups C and IC (p=0.02 and p=0.0001, respectively). Tortuosity in IC group was also significantly higher compared to Group C (p=0.01). The tortuosity index (Fig. 8B) manifested by the largest number of retinal ganglion cells was between 1.2–1.3 for Group A, 1.1–1.25 for Group C and 1.15–1.25 for Group IC.

Dendritic spine density—Dendritic spine density, shown in Figure 9, was calculated as the total number of spines divided by the total dendrite length (sp/L). The main effects of treatment on dendritic spine density of the retinal ganglion cells just failed reaching statistical significance ($F_{(2,16)}$= 3.22, p=0.07). Interestingly, it was the IC group that appeared to have a lower spine density compared to the other groups (Fig. 9A). As shown in Figure 6B, there appeared to be a bimodal distribution of spine density for all groups, with one peak within the range between 0–0.005 and a second peak at 0.01–0.015 sp/L, respectively (Fig. 9B).

Dendritic branch angle—The group effect for dendritic branch angle shown in Figure 10 just failed to reach statistical significance ($F_{(2,16)}$ = 3.35, p=0.06). Because soma area (see Fig. 5A) and mean dendritic field area (Fig. 6A) showed effects of alcohol treatment, individual group comparisons were again carried out. This analysis showed that dendritic branch angle was significantly greater in Group A compared to Groups C and IC (p=0.04), although the magnitude of the difference was small. Groups C and IC did not differ significantly in branch angle (p=0.87). In all three groups, the branch angle frequency distribution appeared normal with a peak at 40 to 50 degrees (Fig 10B).

The remainder of the morphological parameters examined were not significantly affected by early postnatal alcohol exposure. These data are presented as supplementary information. Briefly, early postnatal alcohol exposure did not significantly affect the mean number of dendrites (p=0.4), the mean number of branches/dendrite (p=0.6), the mean branch length (internal, p=0.2; terminal, p=0.2), mean dendritic branch order (p=0.4), symmetry (p=0.5) or dendrite diameter (p=0.5).

DISCUSSION

The present study shows that binge-like ethanol exposure in mice during the early postnatal period from PD3 through PD20 affected the developing visual system, including reducing

the numbers of neurons in the retinal ganglion cell layer, altering several morphological features of retinal ganglion cells, and reducing the number of neurons in the dorsolateral medial geniculate nucleus. Pup body weight gain was not affected by alcohol exposure, and this is likely to be due to the fact that alcohol was administered at a relatively low 3 g/kg/day dose in an enriched milk formula, and that the pups remained with their dams and were allowed to suckle. This alcohol dose and this method of alcohol delivery during early postnatal period have been shown not to compromise body weight gain in new born pups (Serbus et al., 1986).

The peak BAC was reached 1–1.5 h after the last ethanol administration for the three ages examined (i.e., PD 3, 10 & 20) with the average BAC between 156–298 mg/dL. This range is above the toxic level shown by other authors to produce damage to the brain and visual system in rodents (Bonthius and West, 1990; Ikonomidou et al., 2000; Livy et al., 2003; Pierce and West, 1986; Tenkova et al., 2003). The amplitude of the BAC was inversely proportional to the pups' age, as shown in Figure 3. This is likely due to the increase in the efficiency of liver alcohol dehydrogenase and the microsomal ethanol oxidizing system resulting in an increase in metabolic tolerance to alcohol with maturation (Bhalla et al., 2005, Krasner et al., 1974).

In this study, the 3 g/kg/day ethanol dose given to mice during the extended postnatal period between PD 3–20 resulted in a significant loss of neurons in the retinal ganglion cell layer with no change in the total retinal area. Loss of ganglion cell layer neurons after ethanol exposure during the early postnatal period has been reported previously in different animal species such as the macaque monkey (Clarren et al., 1990), rat (Pinoza-Duran et al., 1997), chick (Aguilera et al., 2004; Chmielewski et al., 1997) and also in humans (Pinoza-Duran et al., 1997; Strömland and Pinazo-Duran, 2002). The results are consistent with ethanol-induced reductions in the number of optic nerve fibers and decreases in the optic nerve cross-sectional area reported earlier in mice (Ashwell and Zang,1994; Dangata and Kaufman, 1997; Kennedy and Elliott, 1986; Parnell et al., 2006; Parson and Sojita, 1995; Parson et al., 1995), rats (Harris et al., 2000; Pinazo-Duran et al., 1993; Philips et al., 1991; Samoraski et al., 1986), chicks (Tufan et al., 2007) and zebrafish (Dlugos and Rabin,2007; Kashyap et al., 2007). Ethanol-induced cell loss has been shown to be caused by apoptotic cell death due to ethanol toxicity (Ikonomidou et al., 2000; Tenkova et al., 2003). Exposure to alcohol during development may also alter neurotrophin levels and/or function (Climent et al., 2002; Heaton et al., 1999: 2000(a); 2000(b); Parks, et al., 2008), and change expression of neurotropic receptors (Dohrman et al., 1997; Light et al., 2002). Neurotrophins and their receptors are important for the survival and differentiation of neurons in the chick retina (Frade et al., 1999). In the present study, in parallel to the significant loss of retinal output neurons, a decrease in the number of neurons was found in the lateral geniculate nucleus of the thalamus, the major target area of RGCs. This observation is consistent with the results by Tenkova et al. (2003) pointing towards high susceptibility of dLGN neurons to ethanol toxicity at postnatal days PD4 to PD7 in mice. Our results therefore confirm the generalized neurotoxic effects of early postnatal ethanol administration shown earlier in other brain regions including the hippocampus (Barnes and Walker, 1981; Gonzales-Burgos et al., 2006; Miki et al., 2000,2003,2004,2008; Miller, 1995; Moulder et al., 2002; Tran and Kelly, 2003), cerebellum (Goodlett et al., 1990,1997,1998; Goodlett and Eilers,1997; Miki et al., 1999; Thomas et al., 1998), and cerebral cortex (Climent et al., 2002; Han et al., 2005; Jiang et al., 2007; Money and Napper, 2005; Tenkova et al., 2003). However, it is not possible based on the present results to determine whether the loss of neurons in the dLGN is due to direct neurotoxic effects of ethanol, or whether it may be secondary to a reduction in axonal projections from the retina.

Retinas were collected on PD20 when RGCs are reported to display adult cell morphological characteristics (Chalupa and William, 2008 pp 194; Coombs et al., 2007; Diao et al., 2004). For the quantitative analysis of ganglion cell morphologies in control and ethanol-exposed mice, 13 different structural parameters were considered. These parameters have been previously used to classify RGCs (Coombs et al., 2006). In the present study, irrespective of the RGC type, two conventional size measurements, soma area and dendritic field diameter, were affected by neonatal ethanol exposure. In normal mice, these two parameters show a steady growth during the early postnatal retina development, and so the effects of alcohol exposure are particularly striking (Coombs et al., 2007). Another parameter showing a similar developmental trajectory, dendritic branch length, remained unaffected by early postnatal ethanol administration. The reduced size of both soma and dendritic field area support the idea that within a neuron population, soma size may be a good predictor of the volume occupied by the cell's dendritic arbor. These results are in accord with findings by other authors reporting reduction of soma size and dendritic fields of the neurons in the rat oculomotor nucleus (Burrows et. al, 1995), Bergmann glial cells (Perez-Torrero et al., 1997), and cerebellar granule cells (Smith et al., 1986) due to perinatal alcohol exposure.

Two other morphological measurements appeared to be affected by the ethanol intoxication: dendrite tortuosity and the angle at which dendrites branch. In contrast to soma size and the dendritic field area which were reduced in ethanol-exposed subjects, ethanol administration increased dendrite tortuosity and appeared to increase branch angles. In mice, these two latter features reach adult values shortly after birth, and remain relatively unchanged throughout postnatal development (Coombs et al., 2007). A similar developmental pattern is seen in the kitten cerebellar Purkinje cells (Calvet and Calvet, 1984). However, in postnatal dendritic development of Y-like geniculocortical relay neurons in cat (Coleman and Friedlander, 2002), both the branch angle and dendrite tortuosity have been reported to decrease in the course of postnatal development. During normal development of these dLGN relay neurons, these two changes in the dendritic architecture were negatively correlated with the changes in the size of the soma and dendritic field. Similarly, in the present study the changes in the values of this pair of parameters show opposite trends. A decrease in the branch angle has also been observed for hippocampal pyramidal neurons during human fetal development (Paldino and Purpura, 1979). The decrease in the branch angle occurring during neural development would be expected to contribute to an increase in the distance between the dendrite terminal tips and the soma. The straightening of dendritic segments associated with reduced tortuosity would have a similar effect. However, during early stages of retinal development, the meandering of growing fibers may facilitate location of specific cellular targets, which would be more difficult if dendrite elongation took place along a straight trajectory. It has been postulated by some authors that tortuosity might reflect the searching for specific inputs or targets (Stepanyants et al., 2004). It has been also suggested that increased tortuosity represents a morphologic marker of nerve regeneration (Kallinikos et al., 2004). In the present study, ethanol-induced hypoplasia of the RGCs could result in the delayed reduction in both the branch angle and dendrite tortuosity. The increased dendrite tortuosity in RGCs of ethanol-exposed mice may also explain why the dendritic field area of these neurons was significantly smaller despite no changes recorded in the total dendrite length, number of branches and the highest branch order. The lack of ethanol effects on the RGCs' dendrite length and branch number observed in the present study is consistent with the absence of a significant difference in these two parameters in the rat prefrontal cortex after similar neonatal ethanol intoxication, however, in the latter study, spine density was lower in ethanol treated group as compared to control (Whitcher and Klintsova, 2008). In mice, perinatal ethanol exposure covering late pregnancy and the first postpartum week, the time window coinciding with growth and development of dendritic arbors in hippocampus, was reported to cause a marked reduction in the extent of basilar dendrites in CA1 pyramidal neurons as assessed at PD 14 (Davies and Smith, 1981). In rat

hippocampal pyramidal neuronal cultures, six days of ethanol exposure in the medium (i.e., 200, 400 or 600 mg/dl), beginning at the time of plating, was also shown to decrease the total dendrite number and dendritic length (Yanni and Lindsley, 2000). The changes in the dendritic arbor towards a reduction in the number of dendritic branches, and a reduction in the arbor complexity were also observed in the rat oculomotor nucleus on PD15 (Burrows et al., 1995) and in the mouse cerebellar granular cells on PD14 (Smith et al., 1986) following a prenatal ethanol exposure. In contrast to these findings, Qiang and colleagues (2002) reported an increase in the number and length of apical and basilar dendritic branches in the corpus callosum that project to neurons in the rat visual cortex after prenatal alcohol exposure restricted to the second trimester equivalent. These differing results reported in the literature may be due to regional differences in ethanol susceptibility and different timing of ethanol administration. Interestingly, in the present study, RGC dendrite elongation and the decrease in the spine density were observed in the IC group, as compared to both ethanol-exposed and pure control subjects. The change in the morphology of RGC parameters in the intubation control group may be related to the repeated intubation stress the newborn pups were subjected to. In the alcohol group, intubation stress may have been attenuated by the sedative action of ethanol. Retrospective studies on humans and animals suggest that even chronic maternal stress during pregnancy, associated with raised plasma levels of CRH, ACTH and cortisol, may increase the likelihood of morphological and functional abnormalities in the nervous system of ethanol exposed offspring (Weinstock, 2001). It has been demonstrated that corticosteroid receptors are distributed widely throughout the central nervous system and are also present in the developing retina (Gremo and Vernadakis, 1981; Koehler and Moscona, 1975; Zhang et al., 1993). There are, however, relatively few studies examining the effect of perinatal stress on brain morphology and none on the development of the visual system in rodents. The available studies have been focused on the limbic regions of the brain such as hippocampus, anterior cingulate and orbitofrontal cortices, where perinatal stress can result in dendritic atrophy manifested by reduction in spine densities, but also in the dendrite length and complexity of the dendritic trees (Andersen and Teicher, 2004; Bartesaghi and Severi, 2002; Hayashi et al., 1998; Murmu et al., 2006). These results stand in contrast to the dendrite elongation observed in the IC group in the present study.

The decrease in RGC spine density observed in the IC group could be secondary to the increase in the dendrite length and thus fiber surface in this group. On the other hand, the lack of change in the spine number in the alcohol exposed group in this study differs from some earlier reports of a decrease in the spine density after perinatal ethanol administration. For example, a decrease in the spine number was found in the hippocampal pyramidal cells of 30-day-old rat pups exposed to ethanol during gestation through lactation (Gonzalez-Burgos et. al., 2006). Lower spine density was also reported by Whitcher and Klintsova (2008) in the rat prefrontal cortex after a short, neonatal (PD 4–9) exposure to ethanol although in that study no between-group differences in dendritic complexity were noted. However, these discrepant findings may be related to regional differences in ethanol effects on the developing nervous system (e.g., cortex versus dLGN).

There is strong evidence that ethanol-induced brain damage, including adverse changes occurring in the developing visual system, is most pronounced when ethanol is delivered during the brain growth spurt, a critical period characterized by an increased susceptibility to ethanol effects (Tenkova et al., 2003; Tran et al., 2000). This was the reason why in the present study ethanol was administered to new born mouse pups between PD 3–20. It would be interesting to compare our results with potential changes in the developing mouse retina due to fetal ethanol intoxication throughout embryonic days 11–19, the early period of RGC generation and differentiation. However, to our knowledge, there are no such data available. It is also important to correlate the ethanol-induced morphological abnormalities with

functional changes in the visual system (the degree of impairment in visual perception). Reduced visual acuity in one or both eyes, diplopia, hyperopia, myopia and astigmatism have been reported in FAS children (Strömland, 2004). However, no comparative studies on visual perception have been done so far in rodent models of FAS.

In summary, this study provides clear evidence of ethanol toxicity on the development of mouse RGCs during the early postnatal period considered to be equivalent to the human third trimester when the fetal nervous system is particularly susceptibility to the damaging effects of ethanol. The findings also show that early postnatal ethanol intoxication affected RGC development in dissimilar ways. The most affected parameters were soma size and total dendritic field area, both showing decreases, as well as dendrite branch angle and dendrite tortuosity, both showing an increase. Since during normal retinal development, these parameters also show opposite trends, ethanol-induced changes in RGCs' morphology observed in the present study suggest developmental delay rather than permanent damage. To confirm this notion further investigation of retinal morphology in mouse pups at more advanced ages will be required.

Acknowledgments

We would like to thank Dr. Charles R. Goodlett for his assistance in assessment of BACs, and Dr. Sandra J Kelly for the help with the liquid diet formulation. We also thank Dr. Kyoungmi Kim for helpful advice concerning the statistical analysis of the data, and Dr. Jurgen Wenzel for his guidance on histology. This research was supported by grants from the National Eye Institute of the NIH EY003991 and P30EY12576 to Dr. Leo M. Chalupa and partially by the METU research fund BAP-08-11-DPT-2002-K120510 through a METU–UC Davis collaboration. Dr. I. Dursun spent 1.5 years in UC Davis and would like to thank UC Davis for financial support and hospitality.

REFERENCES

Aguilera Y, Ruiz-Gutiérrez V, Prada FA, Martínez JJ, Quesada A, Dorado ME. Alcohol-Induced Lipid and Morphological Changes in Chick Retinal Development. Alcoholism: Clinical and Experimental Research. 2004; 28(5):816–823.

Andersen SL, Teicher MH. Delayed effects of early stress on hippocampal development. Neuropsychopharmacology. 2004; 29(11):1988–1993. [PubMed: 15316569]

Ashwell KW, Zhang LL. Optic nerve hypoplasia in an acute exposure model of the Fetal Alcohol Syndrome. Neurotoxicology and Teratology. 1994; 16(2):161–167. [PubMed: 8052190]

Badea TC, Nathans J. Quantitative analysis of neuronal morphologies in the mouse retina visualized by using a genetically directed reporter. J Comp Neurol. 2004; 480:331–351. [PubMed: 15558785]

Barnes DE, Walker DW. Prenatal ethanol exposure permanently reduces the number of pyramidal neurons in the rat hippocampus. Developmental Brain Research. 1981; 1:333–340.

Bartesaghi R, Severi S. Effects of early environment on field CA3a pyramidal neuron morphology in the guinea-pig. Neuroscience. 2002; 110:475–488. [PubMed: 11906787]

Berman RF, Hannigan JH. Effects of prenatal alcohol exposure on the hippocampus: Spatial behavior, Electrophysiology, and Neuroanatomy. Hippocampus. 2000; 10:94–110. [PubMed: 10706221]

Bhalla S, Kaur K, Akhtar Mahmood A, Mahmood S. Postnatal development of alcohol dehydrogenase in liver & intestine of rats exposed to ethanol *in utero*. The Indian Journal of Medical Research. 2005; 121:39–45. [PubMed: 15713978]

Bonthius DJ, West JR. Alcohol-induced neuronal loss in developing rats: Increased brain damage with binge exposure. Alcoholism: Clinical and Experimental Research. 1990; 14(1):107–118.

Bruce BB, Biousse V, Dean AL, Newman NJ. Neurologic and ophthalmic manifestations of fetal alcohol syndrome. Reviews in Neurological Diseases. 2009; 6(1):13–20. [PubMed: 19367219]

Burrows RC, Shetty AK, Phillips DE. Effects of prenatal alcohol exposure on the postnatal morphology of the rat oculomotor nucleus. Teratology. 1995; 51:318–328. [PubMed: 7482353]

Calvet MC, Calvet J. Computer assisted analysis of HRP labeled and Golgi stained Purkinje neurons. Progress in Neurobiology. 1984; 23:251–272. [PubMed: 6398453]

Chalupa, LM.; Williams, RW. Eye, Retina, and Visual System of The Mouse. Cambridge, Massachusetts London, England: The MIT press; 2008.

Chmielewski CE, Hernandez LM, Quesada A, Pozas JA, Picabea L, Prada FA. Effects of ethanol on the inner layers of chick retina during development. Alcohol. 1997; 14(4):313–317. [PubMed: 9209545]

Clarren SK, Alvord EC Jr, Sumi SM, Streissguth AP, Smith DW. Brain malformations related to prenatal exposure to ethanol. The Journal of Pediatrics. 1978; 92(1):64–67. [PubMed: 619080]

Clarren SK, Astley SJ, Bowden DM, Lai H, Milam AH, Rudeen PK, Shoemaker WJ. Neuroanatomic and neurochemical human primate infants exposed abnormalities in nonto weekly doses of ethanol during gestation. Alcoholism: Clinical and Experimental Research. 1990; 14(5):674–683.

Climent E, Pascual M, Renau-Piqueras J, Guerri C. Ethanol Exposure Enhances Cell Death in the Developing Cerebral Cortex: Role of Brain- Derived Neurotrophic Factor and Its Signaling Pathways. Journal of Neuroscience Research. 2002; 68:213–225. [PubMed: 11948666]

Coleman LA, Friedlander MJ. Postnatal dendritic development of Y-like geniculocortical relay neurons. International Journal of Developmental Neuroscience. 2002; 20:137–159. [PubMed: 12175851]

Cook CS, Nowotny AZ, Sulik KK. Fetal alcohol syndrome. Eye malformations in a mouse model. Archives of Ophthalmology. 1987; 105(11):1576–1581. [PubMed: 3675291]

Coombs JL, Van Der List D, Wang GY, Chalupa LM. Morphological properties of mouse retinal ganglion cells. Neuroscience. 2006; 140:123–136. [PubMed: 16626866]

Coombs JL, Van Der List D, Chalupa LM. Morphological properties of mouse retinal ganglion cells during postnatal development. The Journal of Comparative Neurology. 2007; 503(6):803–814. [PubMed: 17570502]

Dangata YY, Kaufman MH. Morphometric analysis of the postnatal mouse optic nerve following prenatal exposure to alcohol. Journal of Anatomy. 1997; 191:49–56. [PubMed: 9279658]

Davies DL, Smith DE. A Golgi study of mouse hippocampal CA1 pyramidal neurons following perinatal ethanol exposure. Neuroscience Letters. 1981; 26(1):49–54. [PubMed: 7290537]

Diao L, Sun W, Deng Q, He S. Development of the mouse retina: emerging morphological diversity of the ganglion cells. Journal of Neurobiology. 2004; 61(2):236–249. [PubMed: 15389605]

Dlugos CA, Rabin RA. Ocular deficits associated with alcohol exposure during zebrafish development. The Journal of Comparative Neurology. 2007; 502:497–506. [PubMed: 17394139]

Dobbing J, Sands J. Comparative aspects of the brain growth spurt. Early Human Development. 1979; 311:79–33. [PubMed: 118862]

Dohrman DP, West JR, Pantazis NJ. Ethanol reduces expression of the nerve growth factor receptor, but not nerve growth factor protein levels in the neonatal rat cerebellum. Alcoholism: Clinical and Experimental Research. 1997; 21(5):882–893.

Feng G, Mellow RH, Bernstein M, Keller-Peck C, Nguyen QT, Wallace M, Nerbonne JM, Lichtman JW, Sanes JR. Imaging neuronal subsets in transgenic mice expressing multiple spectral variants of GFP. Neuron. 2000; 28:41–51. [PubMed: 11086982]

Frade JM, Bovolenta P, Rodriguez-Tebar A. Neurotrophins and other growth factors in the generation of retinal neurons. Microscopy Research and Technique. 1999; 45:243–251. [PubMed: 10383117]

Gonzalez-Burgos I, Alejandre-Gomez M, Olvera-Cortes ME, Perez-Vega MI, Evans S, Feria-Velasco A. Prenatal-through-postnatal exposure to moderate levels of ethanol leads to damage on the hippocampal CA1 field of juvenile rats A stereology and golgi study. Neuroscience Research. 2006; 56:400–408. [PubMed: 16978724]

Goodlett CR, Marcussen BL, West JR. A Single Day of Alcohol Exposure During the Brain Growth Spurt Induces Brain Weight Restriction and Cerebellar Purkinje Cell Loss. Alcohol. 1990; 7:107–114. [PubMed: 2328083]

Goodlett CR, Eilers AT. Alcohol-induced purkinje cell loss with a single binge exposure in neonatal rats: A stereological study of temporal windows of vulnerability. Alcoholism: Clinical and Experimental Research. 1997; 21(4):738–744.

Goodlett CR, Pearlman AD, Lundahl KR. Binge-like alcohol exposure of neonatal rats via intragastric intubation induces both Purkinje cell loss and cortical astrogliosis. Alcoholism: Clinical and Experimental Research. 1997; 21(6):1010–1017.

Goodlett CR, Pearlman AD, Lundahl KR. Binge neonatal alcohol intubations induce dose-dependent loss of Purkinje cell. Neurotoxicology and Teratology. 1998; 20(3):285–292. [PubMed: 9638686]

Green JT, Arenos JD, Dillon CJ. The effects of moderate neonatal ethanol exposure on eyeblink conditioning and deep cerebellar nuclei neuron numbers in the rat. Alcohol. 2006; 39(3):135–150. [PubMed: 17127133]

Gremo F, Vernadakis A. Preferential accumulation of [^{3}H] corticosterone in chick brain during embryonic development. Neurochemical Research. 1981; 6(4):343–351. [PubMed: 7266744]

Guerri C. Mechanisms involved in central nervous system dysfunctions induced by prenatal ethanol exposure. Neurotoxicity Research. 2002; 4(4):327–335. [PubMed: 12829422]

Han JY, Joo Y, Kim YS, Lee YK, Kim HJ, Cho GJ, Choi WS, Kang SS. Ethanol induces cell death by activating caspase-3 in the rat cerebral cortex. Molecules and Cells. 2005; 20(2):189–195. [PubMed: 16267392]

Harris SJ, Wilce P, Bedi KS. Exposure of rats to a high but not low dose of ethanol during early postnatal life increases the rate of loss of optic nerve axons and decreases the rate of myelination. Journal of Anatomy. 2000; 197:477–485. [PubMed: 11117631]

Hayashi A, Nagaoka M, Yamada K, Ichitani Y, Miake Y, Okado N. Maternal stress induces synaptic loss and developmental disabilities of offspring maternal stress. International Society for Developmental Neuroscience. 1998; 16(3–4):209–216.

Heaton MB, Mitchell JJ, Paiva M. Ethanol-Induced Alterations in Neurotrophin Expression in Developing Cerebellum: Relationship to Periods of Temporal Susceptibility. Alcoholism: Clinical and Experimental Research. 1999; 23(10):1637–1642.

Heaton MB, Mitchell JJ, Paiva M. Overexpression of NGF Ameliorates Ethanol Neurotoxicity in the Developing Cerebellum. Journal of Neurobiology. 2000a; 45(2):95–104. [PubMed: 11018771]

Heaton MB, Mitchell JJ, Paiva M, Walker DW. Ethanol-induced alterations in the expression of neurotrophic factors in the developing rat central nervous system. Developmental Brain Research. 2000b; 121:97–107. [PubMed: 10837897]

Helfer JL, Calizo LH, Dong WK, Goodlett CR, Greenough WT, Klintsova AY. Binge-like postnatal alcohol exposure triggers cortical gliogenesis in adolescent rats. The Journal of Comparative Neurology. 2009; 514:259–271. [PubMed: 19296475]

Jeon CJ, Strettoi E, Masland RH. The major cell populations of the mouse retina. Journal of Neuroscience. 1998; 18:8936–8946. [PubMed: 9786999]

Jiang Q, Hu Y, Wu P, Cheng X, Li M, Yu D, Deng J. Prenatal alcohol exposure and the neuroapoptosis with long-term effect in visual cortex of mice. Alcohol & Alcoholism. 2007; 42(4): 285–290. [PubMed: 17537831]

Jones KL, Smith DW. Recognition of the fetal alcohol syndrome in early infancy. Lancet. 1973; 2(7836):999–1001. [PubMed: 4127281]

Jones K, Smith D, Ulleland C, Streissguth A. Pattern of malformation in offspring of chronic alcoholic mothers. Lancet. 1973; 1:1267–1272. [PubMed: 4126070]

Ikonomidou C, Bittigau P, Ishimaru MJ, Wozniak DF, Koch C, Genz K. Ethanol-induced apoptotic neurodegeneration and fetal alcohol syndrome. Science. 2000; 287:1056–1060. [PubMed: 10669420]

Kallinikos P, Berhanu M, O'Donnell C, Boulton AJM, Efron N, Malik RA. Corneal Nerve Tortuosity in Diabetic Patients with Neuropathy. Investigative Ophthalmology & Visual Science. 2004; 45(2):418–422. [PubMed: 14744880]

Kashyap B, Frederickson LC, Stenkamp DL. Mechanisms for persistent microphthalmia following ethanol exposure during retinal neurogenesis in zebrafish embryos. Visual Neuroscience. 2007; 24(3):409–421. [PubMed: 17640445]

Kelly SJ, Lawrence CR. "Intragastric intubation of alcohol during the perinatal period". Methods in Molecular Biology. 2008; 447:101–110. [PubMed: 18369914]

Kennedy LA, Elliott MJ. Ocular changes in the mouse embryo following acute maternal ethanol intoxication. Int. J. Devl. Neurosci. 1986; 4(4):311–317.

Koehler DE, Moscona AA. Corticosteroid receptors in the neural retina and other tissues of the chick embryo. Archives of Biochemistry and Biophysics. 1975; (1):102–113. [PubMed: 240318]

Kong JH, Fish DR, Rockhill RL, Masland RH. Diversity of ganglion cells in the mouse retina: Unsupervised morphological classification and its limits. The Journal of Comparative Neurology. 2005; 489(3):293–310. [PubMed: 16025455]

Krasner J, Eriksson M, Yaffe SJ. Developmental changes in mouse liver alcohol dehydrogenase. Biochemical Pharmacology. 1974; 23(3):519–522. [PubMed: 4822739]

Lemoine P, Harousseau H, Borteyru JP, Menuet JC. Children of alcoholic parents: Abnormalities observed in 127 cases. Ouest Medical. 1968; 8:476–482.

Light KE, Brown DP, Newton BW, Belcher SM, Kane CJM. Ethanol-induced alterations of neurotrophin receptor expression on Purkinje cells in the neonatal rat cerebellum. Brain Research. 2002; 924:71–81. [PubMed: 11743997]

Livy DJ, Miller EK, Maier SE, West JR. Fetal alcohol exposure and temporal vulnerability: effects of binge-like alcohol exposure on the developing rat hippocampus. Neurotoxicology and Teratology. 2003; 25:447–458. [PubMed: 12798962]

Matsui JI, Egana AL, Sponholtz TR, Adolph AR, Dowling JE. Effects of ethanol on photoreceptors and visual function in developing zebrafish. Investigative Ophthalmology & Visual Science. 2006; 47(10):4589–4597. [PubMed: 17003456]

Miki T, Harris S, Wilce PA, Takeuchi Y, Bedi KS. The effect of the timing of ethanol exposure during early postnatal life on total number of Purkinje cells in rat cerebellum. J. Anatomy. 1999; 194:423–431.

Miki T, Harris SJ, Wilce PA, Takeuchi Y, Bedi KS. Neurons in the hilus region of the rat hippocampus are depleted in number by exposure to alcohol during early postnatal life. Hippocampus. 2000; 10:284–295. [PubMed: 10902898]

Miki T, Harris SJ, Wilce PA, Takeuchi Y, Bedi KS. Effects of alcohol exposure during early life on neuron numbers in the rat hippocampus. I.Hilus Neurons and Granule Cells. Hippocampus. 2003; 13:388–398. [PubMed: 12722979]

Miki T, Harris SJ, Wilce PA, Takeuchi Y, Bedi KS. Effects of age and alcohol exposure during early life on pyramidal cell numbers in the CA1–CA3 region of the rat hippocampus. Hippocampus. 2004; 14:124–134. [PubMed: 15058490]

Miki T, Yokoyama T, Sumitani K, Kusaka T, Warita K, Matsumoto Y, Wang Z, Wilce PA, Bedi SK, Itoh S, Takeuchi Y. Ethanol neurotoxicity and dentate gyrus development. Congenital Anomalies. 2008; 48:110–117. [PubMed: 18778455]

Miller MW. Generation of neurons in the rat dentate gyrus and hippocampus: Effects of prenatal and postnatal treatment with ethanol. Alcoholism: Clinical and Experimental Research. 1995; 19(6): 1500–1509.

Mooney SM, Napper RM. Early postnatal exposure to alcohol reduces the number of neurons in the occipital but not the parietal cortex of the rat. Alcoholism:Clinical and Experimental Research. 2005; 29(4):683–691.

Mooney SM, Miller MW. Time-specific effects of ethanol exposure on cranial nerve nuclei: Gastrulation and neuronogenesis. Experimental Neurology. 2007; 205(1):56–63. [PubMed: 17320867]

Moulder KL, Fu T, Melbostad H, Cormier RJ, Isenberg KE, Zorumski CF, Mennerick S. Ethanol-induced death of postnatal hippocampal neurons. Neurobiology of Disease. 2002; 10:396–409. [PubMed: 12270700]

Murmu MS, Salomon S, Biala Y, Weinstock M, Braun K, Bock J. Changes of spine density and dendritic complexity in the prefrontal cortex in offspring of mothers exposed to stress during pregnancy. European Journal of Neuroscience. 2006; 24:1477–1487. [PubMed: 16965544]

Paldino AM, Purpura DP. Branching patterns of hippocampal neurons of human fetus during dendritic differentiation. Experimental Neurology. 1979; 64(3):620–631. [PubMed: 467553]

Parks EA, McMechan AP, Hannigan JH, Berman RF. Environmental enrichment alters neurotrophins levels after fetal alcohol exposure in rats. Alcoholism:Clinical and Experimental Research. 2008; 32(10):1741–1751.

Parnell SE, Dehart DB, Wills TA, Chen S, Hodge CW, Besheer J, Waage-Baudet HG, Charness ME, Sulik KK. Maternal oral intake mouse model for fetal alcohol spectrum disorders: Ocular defects as a measure of effect. Alcoholism:Clinical and Experimental Research. 2006; 30(10):1791–1798.

Parson SH, Sojitra NM. Loss of myelinated axons is specific to the central nervous system in a mouse model of the fetal alcohol syndrome. Journal of Anatomy. 1995; 187:739–748. [PubMed: 8586571]

Parson SH, Dhillon B, Findlater GS, Kaufman MH. Optic nerve hypoplasia in the fetal alcohol syndrome: a mouse model. Journal of Anatomy. 1995; 186:313–320. [PubMed: 7649829]

Perez-Torrero E, Duran P, Granados P, Gutierrez-Ospina G, Cintra L, Diaz-Cintra S. Effects of acute prenatal ethanol exposure on Bergmann glia cells early postnatal development. Brain Research. 1997; 746:305–308. [PubMed: 9037511]

Phillips DE, Krueger SK, Rydquist JE. Short- and long-term effects of combined pre-and postnalal ethanol exposure (three trimester equivalency) on the development of myelin and axons in rat optic nerve. Int. J. Devl. Neurosci. 1991; 9:631–647.

Pierce DR, West JR. Alcohol-induced microencephaly during the third trimester equivalent: relationship to dose and blood alcohol concentration. Alcohol. 1986; 3:185–191. [PubMed: 3741615]

Pinazo-Duran MD, Renau-Piqueras J, Guerri C. Developmental changes in the optic nerve related to ethanol consumption in pregnant rats: Analysis of the ethanol-exposed optic nerve. Teratology. 1993; 48:305–322. [PubMed: 8278930]

Pinazo-Duran MD, Renau-Piqueras J, Guerri C, Strömland K. Optic nerve hypoplasia in fetal alcohol syndrome: an update. European Journal of Ophthalmology. 1997; 7(3):262–270. [PubMed: 9352281]

Pons S, Zanon-Moreno V, Melo P, Vila V, Gallego- Pinazo R, Pinazo-Duran MD. Optic neuropathy induced by prenatal drug or alcohol exposure. Arch Soc Esp Oftalmol. 2007; 82:21–26. [PubMed: 17262233]

Qiang M, Wang MW, Elberger AJ. Second trimester prenatal alcohol exposure alters development of rat corpus callosum. Neurotoxicology and Teratology. 2002; 24:719–732. [PubMed: 12460654]

Rice D, Barone S Jr. Critical periods of vulnerability for the developing nervous system: evidence from humans and animal models. Environ Health Perspect. 2000; (3):511–533. [PubMed: 10852851]

Riley EP, Mattson SN, Sowell ER, Jernigan TL, Sobel DF, Jones KL. Abnormalities of the corpus callosum in children prenatally exposed to alcohol. Alcoholism: Clinical and Experimental Research. 1995; 19(5):1198–1202.

Samoraski T, Lancaster F, Wiggins RC. Fetal Ethanol Exposure: A Morphometric Analysis of Myelination in the Optic Nerve. International Journal of Developmental Neuroscience. 1986; 4(4): 369–374. [PubMed: 3455596]

Serbus DC, Young MW, Light KE. Blood ethanol concentrations following intragastric intubation of neonatal rat pups. Neurobehavioral Toxicology and Teratology. 1986; 8(4):403–406. [PubMed: 3762850]

Smith DE, Foundas A, Canale J. Effect of perinatally administered ethanol on the development of the cerebellar granule cell. Experimental Neurololgy. 1986; 92:491–501.

Stepanyants A, Tama´s G, Chklovskii DB. Class-specific features of neuronal wiring. Neuron. 2004; 43:251–259. [PubMed: 15260960]

Streissguth AP, Landesman-Dwyer S, Martin JC, Smith DW. Teratogenic effects of alcohol in humans and laboratory animals. Science. 1980; 209(4454):353–361. [PubMed: 6992275]

Strömland K. Ocular involvement in the fetal alcohol syndrome. Survey of Ophthalmology. 1987; 31(4):277–284. [PubMed: 3107154]

Strömland K, Pinoza-Duran MD. Optic nerve hypoplasia: Comparative effects in children and rats exposed to alcohol during pregnanacy. Teratology. 1994; 50:100–111. [PubMed: 7801297]

Strömland K, Pinoza-Duran MD. Ophthalmic involvement in Fetal Alcohol Syndrome: Clinical and Animal model studies. Alcohol &Alcoholism. 2002; 37(1):2–8. [PubMed: 11825849]

Strömland K. Visual impairment and ocular abnormalities in children with fetal alcohol syndrome Addiction. Biology. 2004; 9:153–157.

Sun W, Li N, He S. Large-scale morphological survey of mouse retinal ganglion cells. Visual Neuroscience. 2002; 19(4):483–493. [PubMed: 12511081]

Tenkova T, Young C, Dikranian K, Labruyere J, Olney JW. Ethanol induced apoptosis in the developing visual system during synaptogenesis. Investigative Ophthalmology & Visual Science. 2003; 44(7):2809–2817. [PubMed: 12824217]

Thomas JD, Goodlett CR, West JR. Alcohol-induced Purkinje cell loss depends on developmental timing of alcohol exposure and correlates with motor performance. Developmental Psychobiology. 1998; 29(5):433–452. [PubMed: 8809494]

Tran TD, Cronise K, Marino MD, Jenkins WJ, Kelly SJ. Critical periods for the effects of alcohol exposure on brain weight, body weight, activity and investigation. Behavioural Brain Research. 2000; 116:99–110. [PubMed: 11090889]

Tran TD, Kelly SJ. Critical periods for ethanol-induced cell loss in the hippocampal formation. Neurotoxicology and Teratology. 2003; 25:519–528. [PubMed: 12972065]

Tufan AC, Abbana C, Akdogan I, Erdogan D, Ozogul C. The effect of in ovo ethanol exposure on retina and optic nerve in a chick embryo model system. Reproductive Toxicology. 2007; 23:75–82. [PubMed: 17074462]

Weinstock M. Alterations induced by gestational stress in brain morphology and West MJ New stereological methods for counting neurons. Neurobiology of Aging. 2001; 14:275–285. 1993.

Whitcher LT, Klintsova AY. Postnatal binge-like alcohol exposure reduces spine density without affecting dendritic morphology in rat mPFC. Synapse. 2008; 62(8):566–573. [PubMed: 18512209]

Yanni PA, Lindsley TA. Ethanol inhibits development of dendrites and synapses in rat hippocampal pyramidal neuron cultures. Brain Res Dev Brain Res. 2000; 120(2):233–243.

Zhang H, Li YC, Young AP. Protein kinase A activation of glucocorticoid-mediated signaling in the developing retina. Proceedings of the National Academy of Sciences of the U S A. 1993; 90(9): 3880–3884.

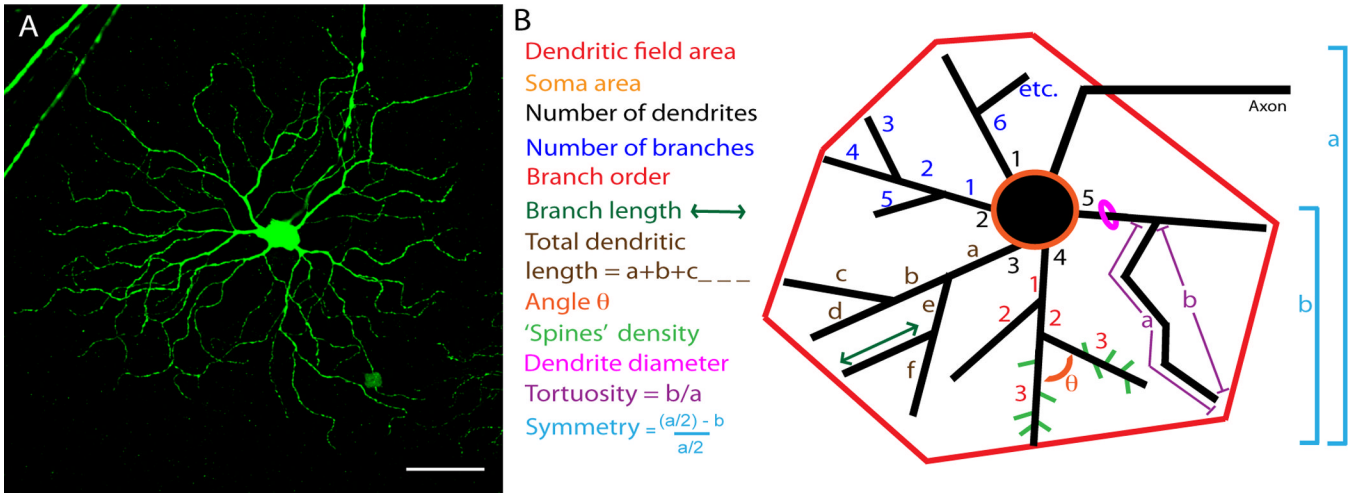

Figure 1.

(A) Photomicrograph of retinal ganglion cell expressing yellow fluorescent protein (bar = 50 microns). (B) Diagramatic representation of the 13 morphological parameters measured on each RGC (see text for details).

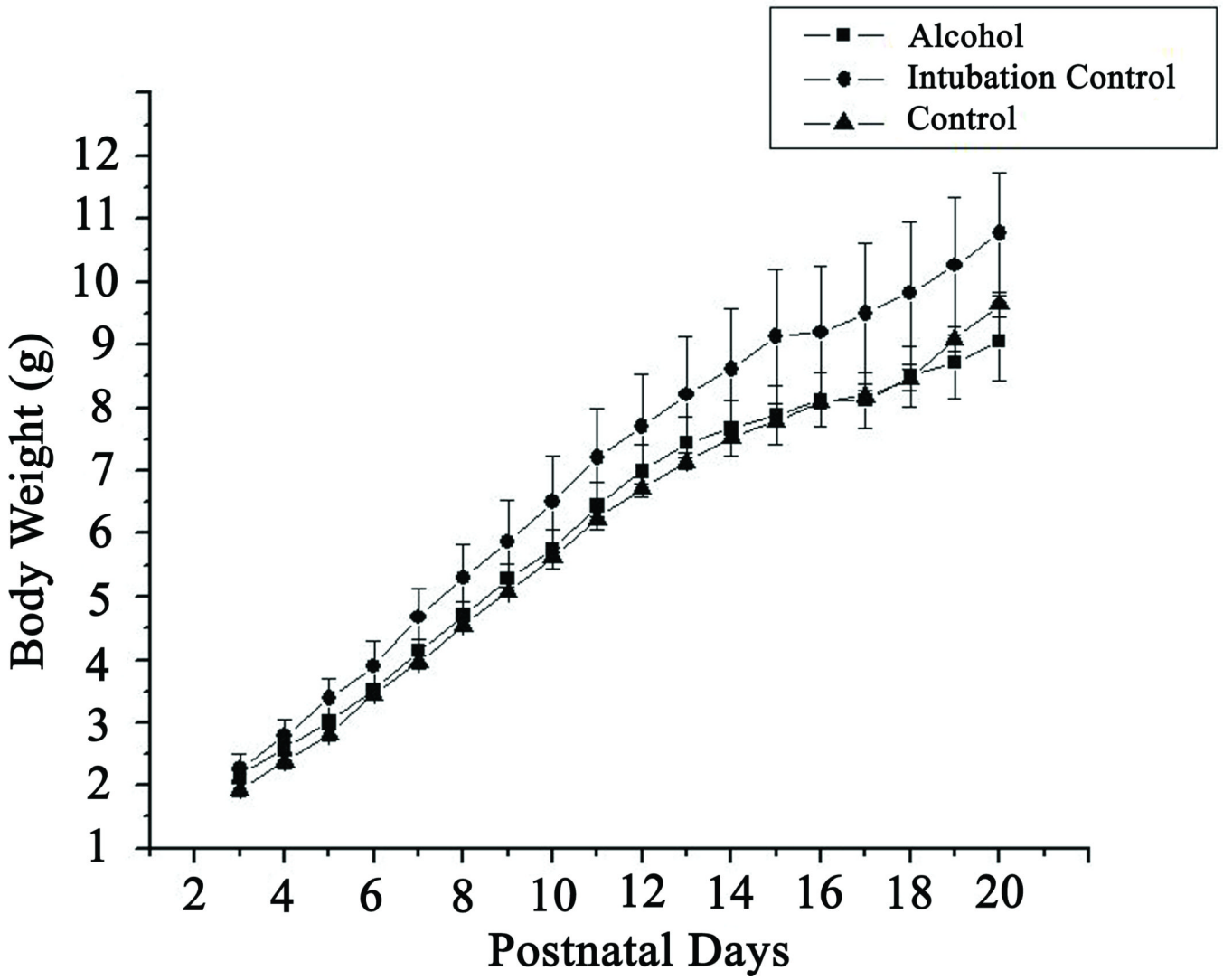

Figure 2.
Growth rates of the three treatment groups, A, IC, and C, with daily body weights averaged across male and female pups in each group. Error bars denote SEM.

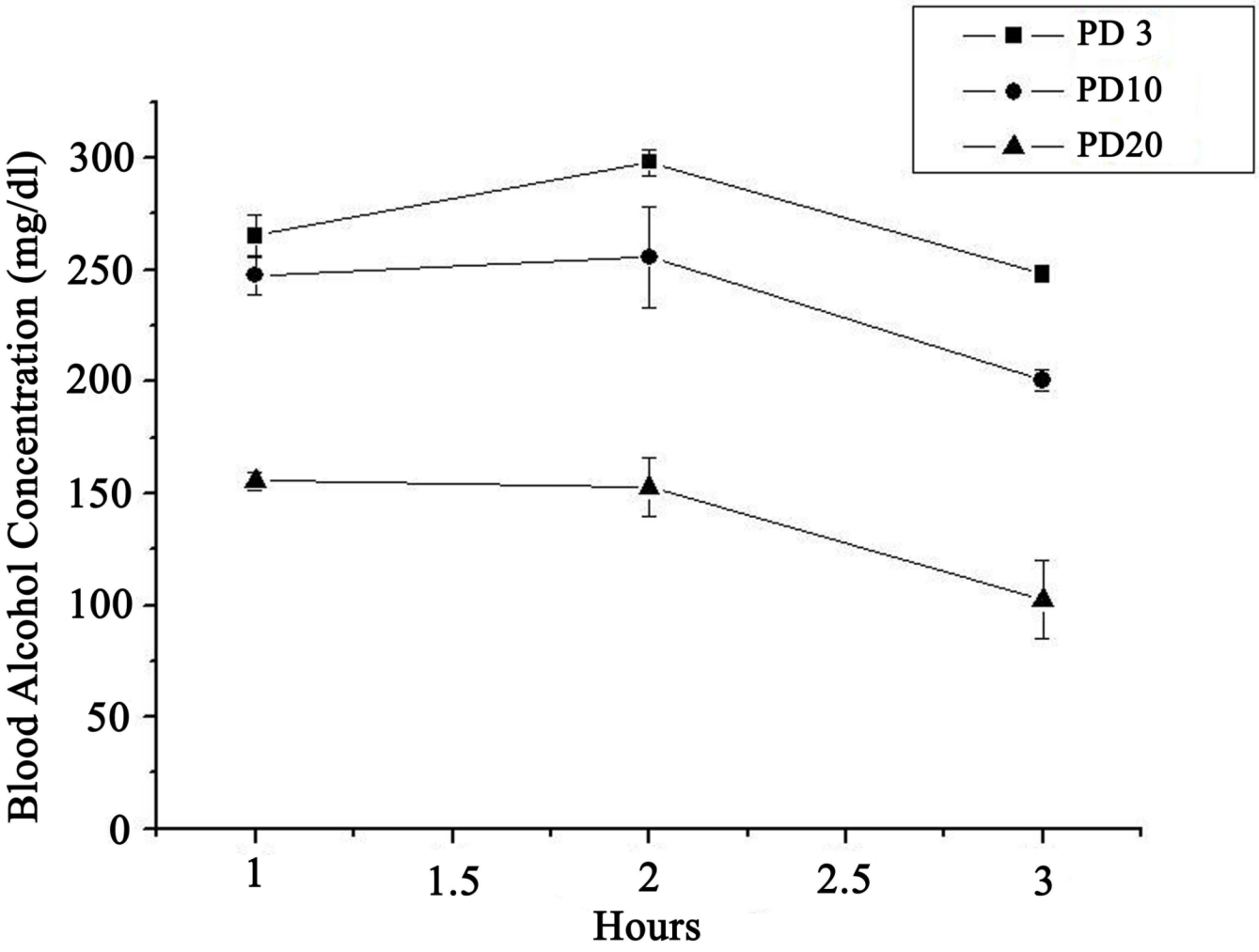

Figure 3.
Mean of blood alcohol concentration measured 1, 1.5, 2, 3 hour following last intubation with alcohol containing milk on PD3, PD10 and PD20. Error bars denote SEM.

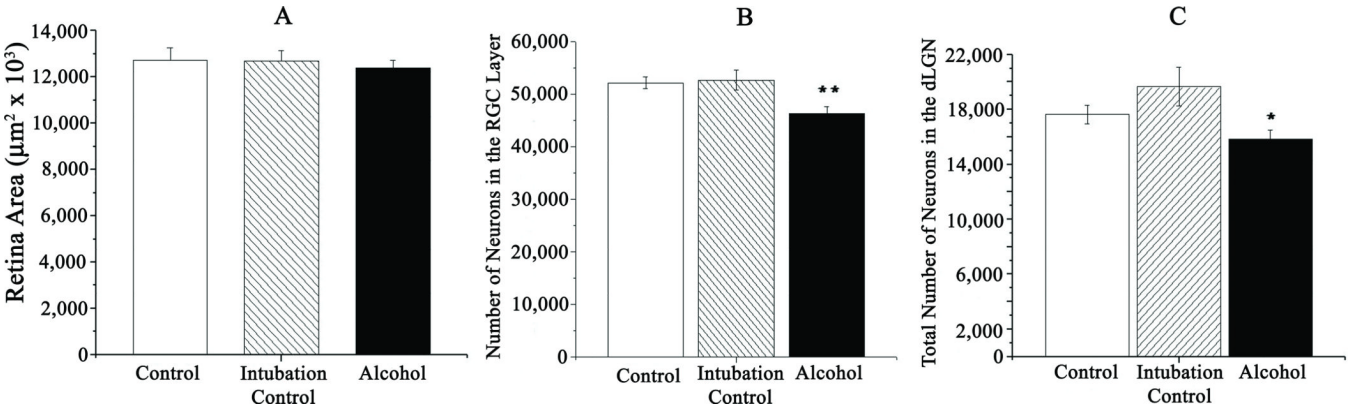

Figure 4.

The total retina area (A), the mean number of neurons in the retinal ganglion cell layer (B) and total number of neurons in the dLGN estimated at P20 (C). Error bars denote SEM. *p<0.05

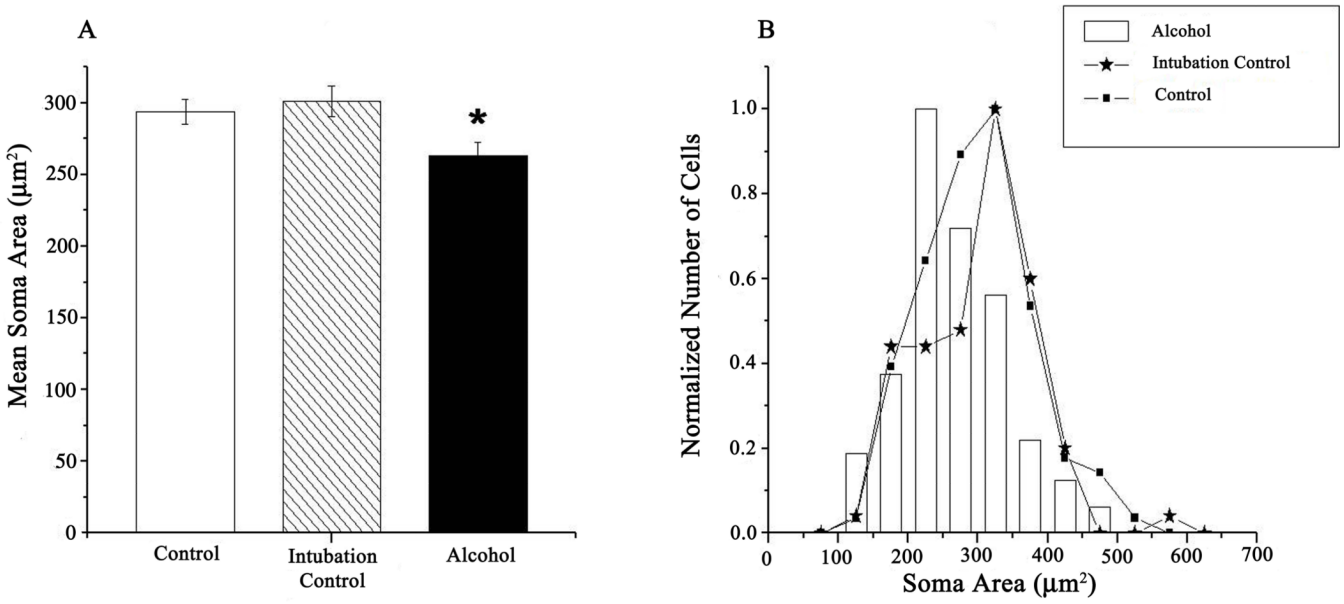

Figure 5.
Morphometric measures of Soma Area (A) and the normalized distribution of ganglion cells (B). Error bars denote SEM. *p<0.05

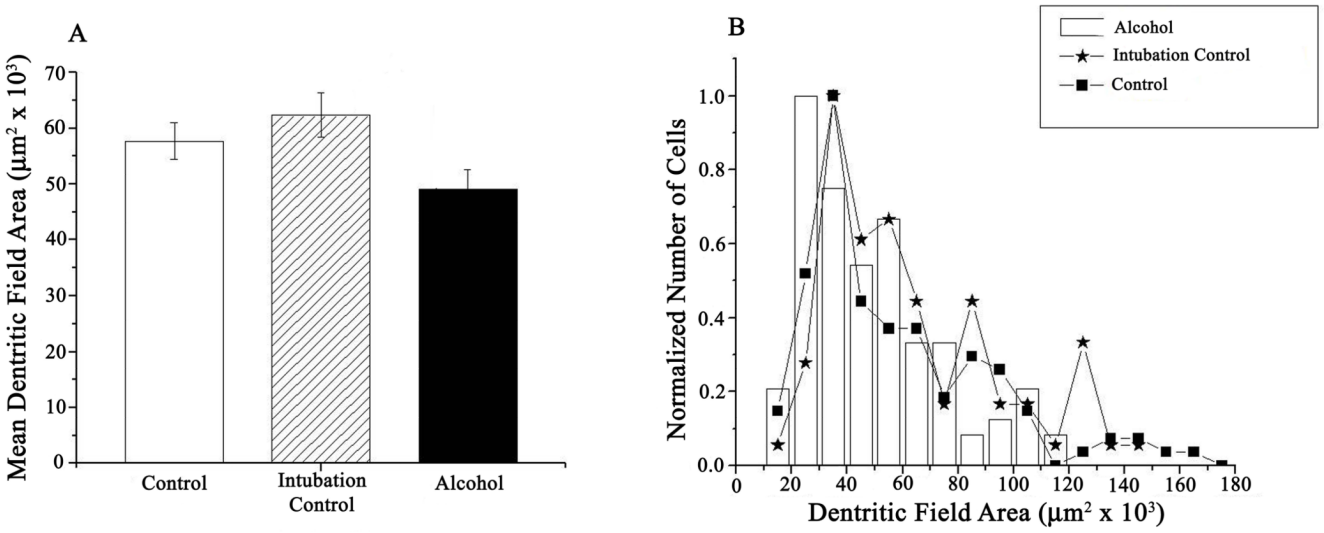

Figure 6.
Morphometric measures of Dentritic Field Area (A) and the normalized distribution of ganglion cells (B). Error bars denote SEM. *p=0.02

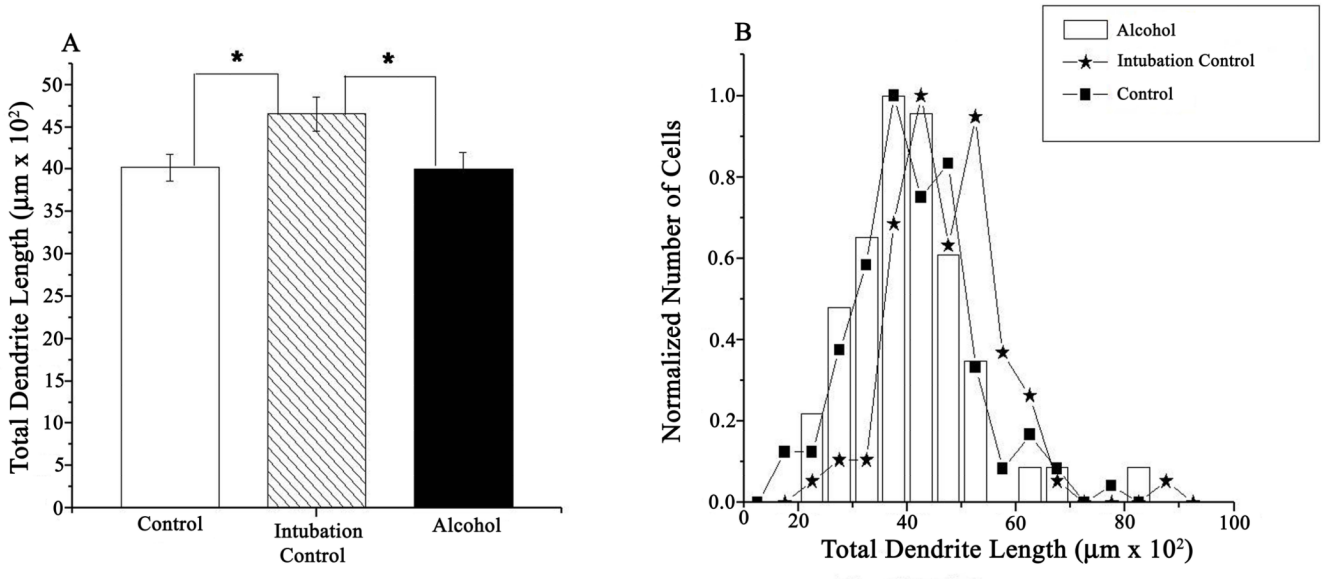

Figure 7.
Morphometric measures of Total Dentritic Length (A) and the normalized distribution of ganglion cells (B). Error bars denote SEM. *p<0.05

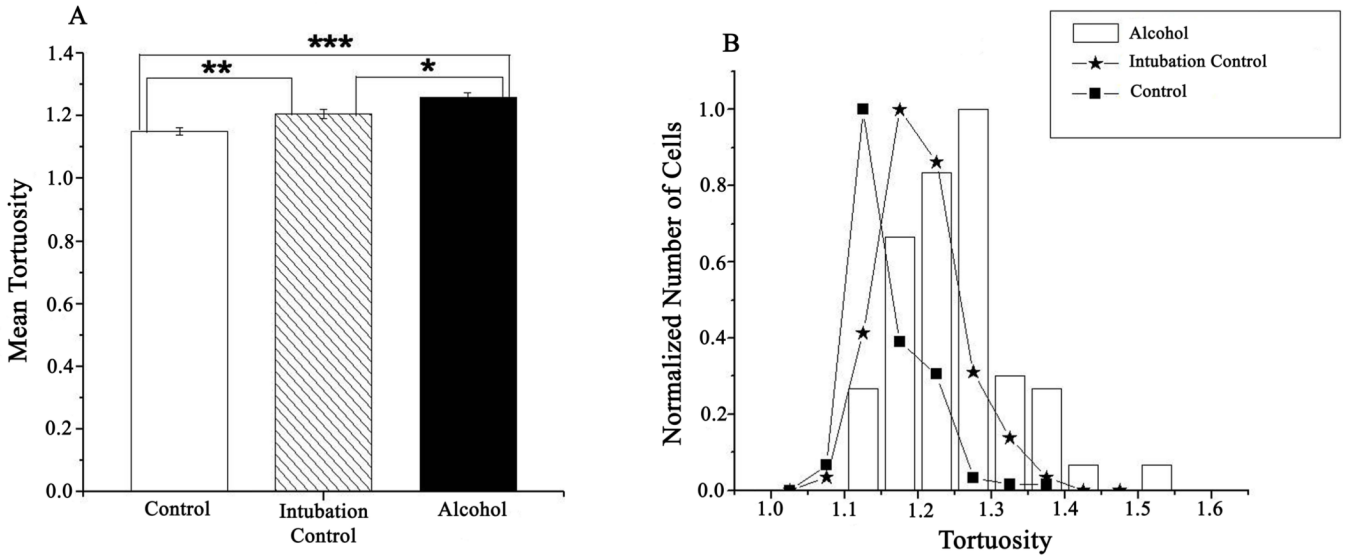

Figure 8.

Morphometric measures of Tortuosity (A) and the normalized distribution of ganglion cells (B). Error bars denote SEM. *p<0.05, **p<0.01, ***p<0.001.

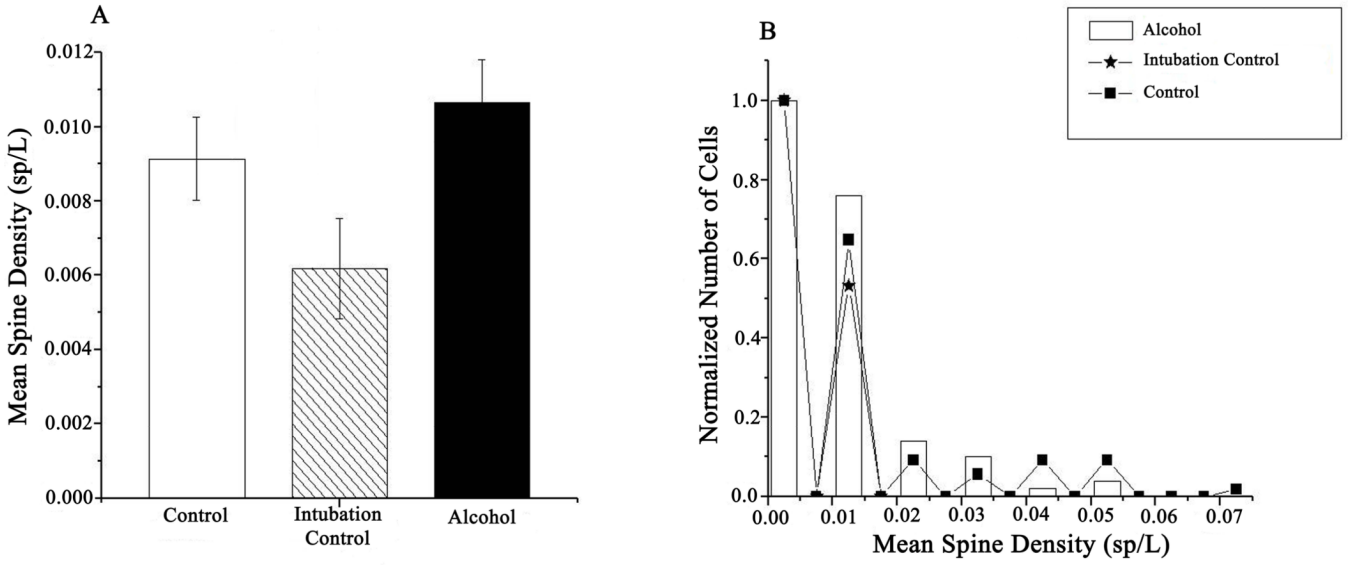

Figure 9.
Morphometric measures of Spine Density (A) and the normalized distribution of ganglion cells (B). Error bars denote SEM.

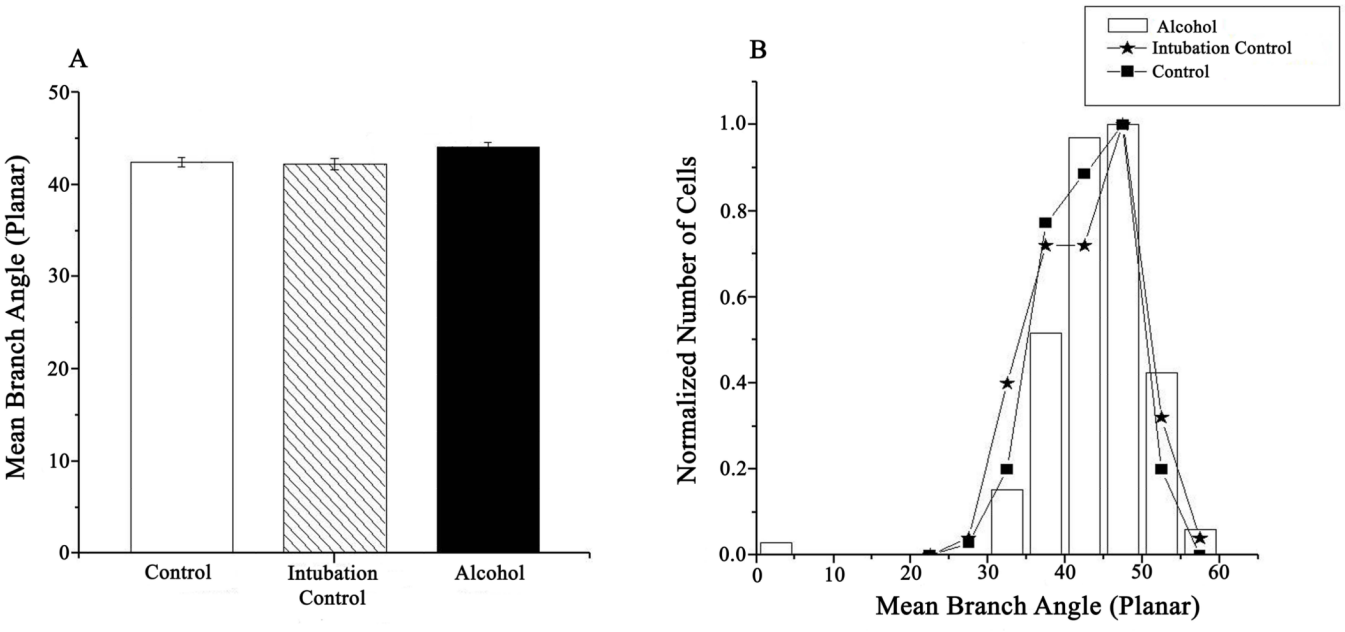

Figure 10.
Morphometric measures of Branch Angle (A) and the normalized distribution of ganglion cells (B). Error bars denote SEM. *p=0.04